PRF#: 58471 DNI 9

Understanding Fracture Permeability Evolution During Enhanced Oil Recovery (EOR)

PI: Lauren E. Beckingham
Department of Civil Engineering, Auburn University, Auburn, AL 36830

The goal of this work is to enhance understanding of the evolution of fracture and formation properties due to geochemical reactions in CO_2-enhanced oil recovery systems. When CO_2 is used to enhance oil recovery, it can dissolve into formation brine, lowering pH and creating conditions favorable for dissolution of primary minerals. As reactions progress, the pH can be buffered by carbonate mineral dissolution and create conditions favorable for precipitation of secondary minerals. These mineral reactions may occur on fracture surfaces or in the low permeability matrix adjacent to fractures and will impact fracture permeability. Here, we aim to enhance understanding of these reactions in fractures and the adjacent matrix and the corresponding evolution of fracture and matrix permeability. Towards this goal, we are first evaluating the role of mineralogy in controlling fracture formation.

Fracturing and characterization of shale core samples

Sample description

The samples used for this project are from the Marcellus formation (northeastern US) and the Mancos formation (mid-western US). Samples were obtained from Kocurek Industries in the form of 1" by 2" cores, where four are Mancos shale and seven are Marcellus shale. The expected mineralogy, shown in Table 1, was provided by Kocurek Industries via X-ray diffraction analysis. Individual mineral strength, as based on Moh's hardness scale, indicate that clay and carbonate minerals are the weakest phases in these samples. Specifically, kaolinite, muscovite, calcite, and dolomite, in order of weakest (clay) to strongest (carbonate), suggesting that these mineral phases are where fractures are most likely to occur.

Table 1: Anticipated sample composition provided (Kocurek Industries) and Moh's hardness for each phase.

	Quartz	Muscovite	Calcite	Dolomite	Microcline	Albite	Kaolinite	Pyrite
Moh's Hardness	7	2.5	3	3.5 - 4	6	6 – 6.5	2 – 2.5	6 - 6.5
Marcellus composition (wt%)	45.9	15.3	26.6	4.0	1.4	2.8	1.2	2.8
Mancos composition (wt%)	56.4	9.7	5.1	10.9	7.9	6.4	2.5	1.1

Fracturing of samples

To induce fractures, the cores were subjected to unconfined compression, as shown in Figure 1. To ensure even distribution of the applied load, the ends of the cores were first made level by sanding. The first fracture tests were performed on four Marcellus cores (Figure 1). Test 1 required two loading cycles before a single fracture formed. Loading for tests 2-4 resulted the cores being crushed into many pieces (Figure 2b). In an attempt to preserve the initial fracture propagation, subsequent compression tests were stopped after initial fracturing occurred. This resulted in distinct initial fracture surfaces for thre remaining Mancos and Marcellus samples, examples shown in Figure 2. However, because this fracture method varies for each sample, the compression data collected is not representative of true specimen strengths and thus is not reported.

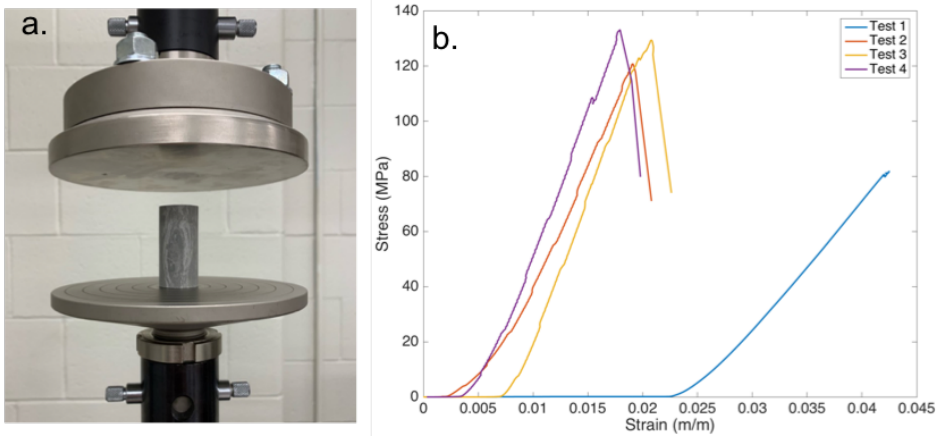

Figure 1: Unconfined compression test method featuring Mancos core (a) and measured Marcellus strain data (b) for four different test specimens.

Assessment of the relationship between mineralogy and fracture formation

Mineral identification

To determine the composition of minerals on the fracture surface, 2D scanning electron microscopy (SEM) backscattered electron (BSE) and energy dispersive spectroscopy (EDS) images were taken of the first Marcellus sample (Figure 2a). Images were collected on the uncoated fracture surface under low pressure (Figure 3). MATLAB codes were then created and used to process images and distinguish individual mineral phases, ultimately creating a mineral map where each color pixel corresponds to a different mineral phase (Figure 3). Figure 3 shows the original BSE image, select EDS images, and the resulting mineral map. This map was then used to quantify volume fractions of each phase and porosity by pixel counting (Table 2). In this sample, the fracture surface is predominantly calcite in spite of an average composition of only 26.6 wt% calcite (Table 1). Additional imaging work is currently underway to consider mineral distributions on additional fracture surfaces for both samples.

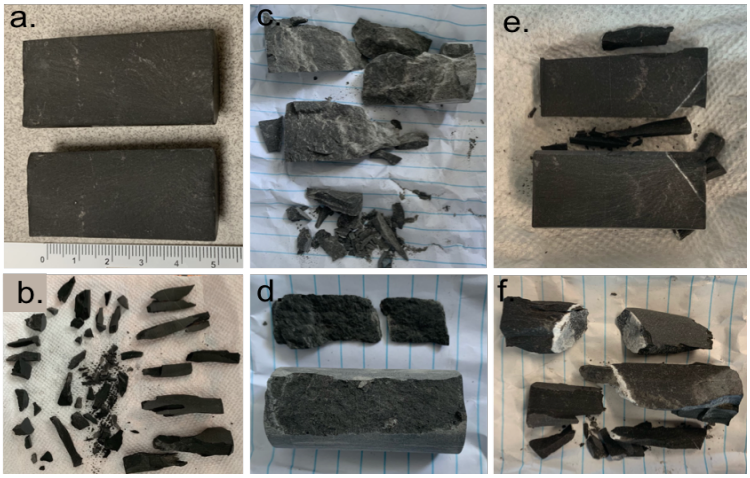

Figure 2: Examples of fractured samples including first test on Marcellus samples (a, b), where (a) was used for imaging. Fractured Marcellus (c, d) and Mancos (e, f) samples where loading stopped after initial fracturing.

Table 2: Mineral abundances (vol. %) for a Marcellus sample determined from processes SEM image (Figure 3).

Phase	Quartz	Muscovite	Calcite	Dolomite	Microcline	Albite	Kaolinite	Pyrite	Carbon	Other	Porosity
Vol. %	2.91	0.51	93.46	0.05	0	0	1.28	0.50	0.32	0.72	0.25

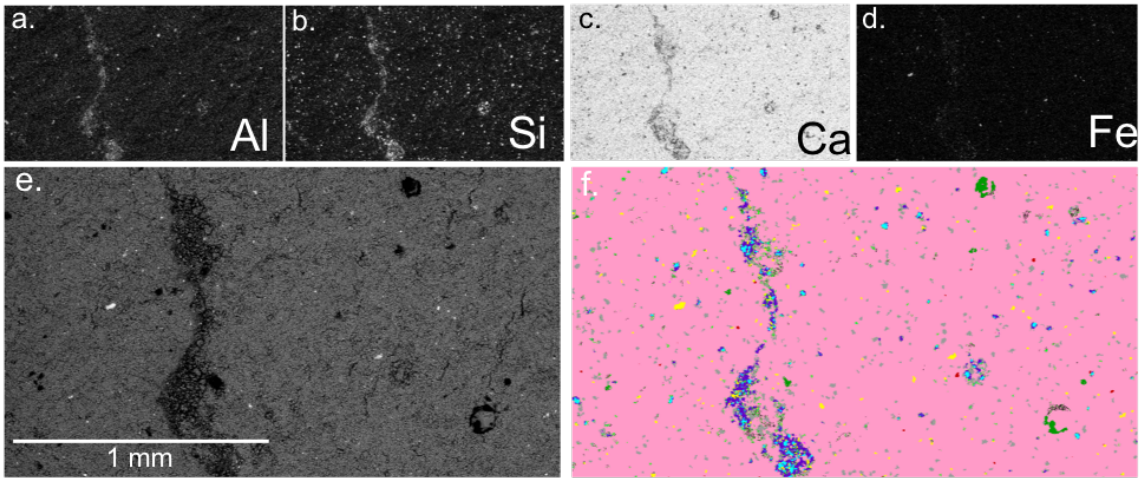

Figure 3: SEM EDS elemental maps (a-d), BSE image (e and processed mineral map (f) of fractured Marcellus sample where pink is calcite, gray is quartz, yellow is pyrite, green is carbon, red is dolomite, purple is kaolinite and cyan is muscovite.

Impact of research

The support provided by the ACS PRF DNI award has allowed the PI to expand the work of her research group to consider new sample types (shales), new reactive geometries (fractures, nano-pore matrices), and new application areas (EOR). This has also resulted in new expertise in sample analysis (compression testing). The resulting associated work has resulted in participation of the PI and involved student in a regional research symposium focused on CO_2 capture, utilization and storage in the southeastern United States. The involved student presented a poster on her related work at this symposium and has submitted an abstract to present this work at the American Geophysical Union Fall meeting in December 2019.